PROCEEDINGS OF SCIENCE

First Year Results from the ALICE Experiment

P.G. Kuijer* **for the ALICE collaboration**
Nikhef, National Institute for Subatomic Physics, Amsterdam, The Netherlands
E-mail: Paul.Kuijer@nikhef.nl

The ALICE experiment has recorded the first pp and PbPb collisions at the LHC during 2010. This article presents an overview of the first results from measurements of pp and PbPb collisions.

Workshop on Discovery Physics at the LHC -Kruger 2010
December 05-10, 2010
Kruger National Park, Mpumalanga, South Africa

*Speaker.

PoS(Kruger 2010)007

1. Introduction

The dedicated heavy ion experiment ALICE at the Large Hadron Collider (LHC) is optimized to study matter under extreme conditions of temperature and pressure. This matter, the Quark Gluon Plasma (QGP) is produced in collisions between heavy nuclei (PbPb). With an energy up to 30 times higher than RHIC the LHC is expected to produce a QGP with a larger lifetime, volume and initial temperature. Thus hard signals like jets and heavy quark production become more easily accessible as a tool to study the properties of the QGP.

The study of collisions of other systems like proton-proton (pp) and proton nucleus (pA) is equally important as comparison data for the heavy ion programme. Therefore in addition to the heavy ion collisions, soft QCD processes in Minimum Bias (MB) and high multiplicity pp events are part of the ALICE programme. The ALICE detector was designed to perform well for the detection of low momentum particles making its capabilities complementary to those of the other LHC experiments in these studies. A detailed characterization of global event properties in MB events will also allow tuning of Monte Carlo event generators to better describe the QCD background underlying the signals used for searches for new physics.

In 2009 and 2010 pp data at 0.9 and 7 TeV as well as PbPb data at 2.76 TeV were collected. A sample of high multiplicity pp collisions, reaching multiplicity densities comparable to lower energy heavy ion collisions was obtained with a dedicated trigger. This sample will be used to test if such events are dominated by hard multi-jet final states or if heavy ion like features already appear in pp collisions.

2. The ALICE Detector

ALICE is a general purpose heavy-ion experiment designed to deal with large particle multiplicities, dN/dy up to 8000, well above the measured multiplicities for central PbPb collisions at LHC energies. In addition the detector [1, 2] is optimized to measure low momentum particles with full particle identification.

The ALICE detector consists of a central tracking and particle identification system covering the pseudorapidity range $-0.9 \leq \eta \leq 0.9$, a muon spectrometer covering $-4.0 \leq \eta \leq -2.4$, a forward multiplicity detector and a zero–degree calorimeter as well as trigger detectors (V0, T0) placed around the beam pipe. The central tracking system, which has full azimuth coverage and measures both the time of flight and $\mathrm{d}E/\mathrm{dx}$, is complemented by several detectors with partial azimuth coverage for particle identification at higher momenta.

The central part is embedded in the large L3 solenoidal magnet which provides a field of 0.5 T. The tracking system is subdivided in the inner tracking system (ITS) using different kinds of silicon detectors and a large time projection chamber (TPC) [3]. The inner tracking system consists of six cylindrical layers of detectors. From the inside out the ITS consists of two layers of silicon pixel detectors (SPD), two layers of silicon drift detectors and two layers of silicon strip detectors. The TPC consists of two 2.5 m long drift volumes separated by a central cathode. The inner tracking system determines the vertex resolution of the system while the TPC essentially defines the momentum resolution.

The transition radiation detector and the time of flight (TOF) array cover the full azimuth. Additional detectors with partial coverage of the central barrel are the photon spectrometer, the high momentum particle identification detector and the electromagnetic calorimeter.

Read-out of the muon spectrometer is triggered by the muon trigger chambers. The central tracking system is triggered by a combination of dedicated trigger detectors (T0, V0) placed around the beam-pipe and by a trigger derived from the SPD in the innermost layers of the silicon tracking system. Each chip in the SPD outputs a "fast-or" signal indicating that at least one pixel has fired. These signals are combined in a global multiplicity trigger which can be adjusted to select central collisions in PbPb collisions. However, since the noise in the pixel detectors is intrinsically low, the system was also used to trigger on single particles to collect a minimum bias sample.

The hardware triggering system is complemented by a high level trigger (HLT) system which uses a large processor farm to select or tag events after read-out of the hardware. In addition to its event selection capabilities this system provides a data quality monitoring facility.

Due to the extreme minimization of the material budget of the inner tracking system the transverse momentum cut-off, with full particle identification, is only 0.1 GeV. The transverse momentum measurement reaches up to 50 GeV with particle identification at mid-rapidity. Details of the detector design and the design performance are described in [2].

The ALICE detectors were commissioned before the start of the LHC using cosmic rays and LHC injection tests. The alignment [4] and calibration were further refined using the first recorded collisions. The material budget was measured using electrons from photon conversion in the material of the tracking system. These results were used to tune the Monte-Carlo simulation of the detector system, which is essential to understand the response of the detector. The simulation of the ALICE detector agrees within 5% with the measured material density.

The LHC started operation in November 2009 with pp collisions at 900 GeV and it reached its current maximum energy of 7 TeV in March 2010. The primary goal for pp for ALICE was to collect about 10^9 minimum bias collisions under clean experimental conditions. The experiment was running for much of 2010 in a special low luminosity mode, in which the LHC beams were separated by up-to 5σ in the ALICE interaction region, to keep the event pile-up below a few percent per bunch crossing. At 0.9 TeV and 7.0 TeV the minimum bias trigger required a hit in either the VZERO counters or in the SPD detector, i.e. essentially one charged particle anywhere in the 8 units of pseudorapidity covered by these trigger detectors. This trigger was used in coincidence with the LHC beam pick-up counters (BPTX), one on each side of the interaction region, indicating the presence of passing bunches. The total pp sample collected at 7 TeV(900 GeV) corresponds to about 700 M (7 M) minimum bias triggers, 50 M muon triggers and approximately 20 M high multiplicity triggers. In addition a short test run was taken at 2.36 TeV with a small subset of the detectors being read-out. During this run the trigger required at least one hit in the SPD detector ($|\eta| < 2$) in coincidence with the beam pick-up counters.

The first heavy-ion collisions at 2.76 TeV started in November 2010. The switch-over from pp collisions took only a few days and the accelerator worked exceedingly well also for PbPb beams. The luminosity reached $2 \times 10^{25}\mathrm{cm}^{-2}\mathrm{s}^{-1}$, yielding about 30 M nuclear interactions recorded.

3. Charged particle multiplicity density

For the first data only the information from the two innermost layers of the tracking system (SPD) was used to measure the position of the interaction and the number of produced charged particles. The position of the interaction vertex is determined by correlating the hits in the inner and outer layers of the SPD. The vertex resolution is better than 300 μm in the transverse direction and better than 500 μm in the longitudinal direction. A tracklet is defined by a combination of hits in the inner and out layers which points to the reconstructed. The correction factors for efficiencies and geometrical acceptance were obtained with Monte-Carlo simulations of the detector set-up, applying the same tracklet finding and vertex finding algorithms as those used for the data. Similarly the number of tracklets was corrected for the contamination due to secondary particles, weak decays and photon conversion by using two different event generators, PYTHIA [5] and PHOJET [6].

The charged particle density $\mathrm{dN}/\mathrm{d}\eta$ and the multiplicity distributions were measured [7, 8, 9, 10, 11] using the data from the 0.9 TeV, 2.36 TeV and 7.0 TeV pp runs and the 2.76 TeV PbPb run. The measured values from the pp run were compared to simulations using three different PYTHIA tunes and PHOJET as event generators. The PYTHIA ATLAS-CSC tune is consistent with the 0.9 TeV and 2.36 TeV charged particle pseudorapidity density and only two standard deviations below the 7.0 TeV data. PHOJET is compatible with the 0.9 TeV data only.

The results are normalized to three different event classes. The INEL $> 0_{|\eta|<1}$ event class corresponds most closely to the measured events after background rejection, i.e. requiring at least one charged particle in the pseudorapidity interval $\eta < 1$. For the inelastic (INEL) and non-single diffractive (NSD) event classes the corrections were determined using PYTHIA and PHOJET based simulations.

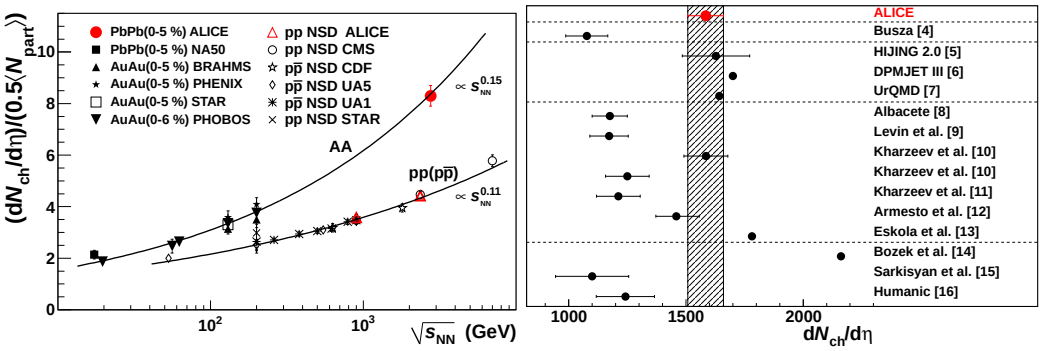

Figure 1: Figures reproduced from [10]. Left panel: Charged particle pseudorapidity density in the central region $|\eta| < 1$ for inelastic collisions as a function of the centre-of-mass energy for pp collisions and for AA collisions (scaled by the number of participants). The lines indicate a fit using a power law dependence on energy. Right panel: Comparison of the pseudorapidity density in the central region with calculations and simulation predictions.

The energy dependence of the multiplicity in pp collisions is described by a power law in energy with an exponent 0.11. The increase with energy is significantly faster than predicted by most event generators. The increase is most pronounced for events with a multiplicity much larger than average.

The measured charged particle multiplicity for the 5% most central PbPb collsions at 2.76 TeV is $dN/d\eta = 1584 \pm 4(\text{stat}) \pm 76(\text{sys})$, corresponding to $8.3 \pm 0.4(\text{sys})$ per participant pair. Figure 1, left panel, compares this measurement to the measurements for AuAu and non single diffractive pp and $p\bar{p}$ collisions. The average multiplicity per participant pair for this centrality selection is a factor 1.9 higher than that for pp and $p\bar{p}$ collisions at similar energies. Figure 1, right panel, compares the measurement to model calculations that describe RHIC measurements and for which predictions for this energy are available. For a more detailed description of this comparison see [10]. The measured

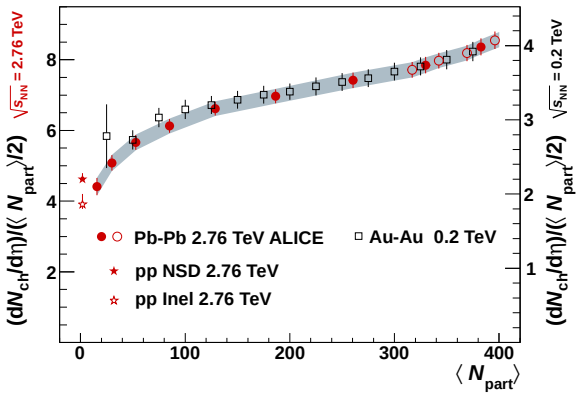

Figure 2: Figure reproduced from [11]. Dependence of $dN_{ch}/(< N_{part} > /2)$ on the number of participants for LHC and RHIC data. The scale for the lower energy data is shown on the right hand side and differs from the scale for the higher energy data on the left hand side by a factor 2.1. For the PbPb data, uncorrelated uncertainties are indicated by the error bars, while correlated uncertainties are shown as the grey band. Statistical errors are negligible. The open circles show the values obtained for centrality classes obtained by dividing the 0-10% most central collisions into four, rather than two classes. The values for non-single-diffractive and inelastic pp collisions are the results of interpolating between data at 2.36 and 7 TeV

multiplicity for central collisions indicates an increase of the energy density by at least a factor three with an increase of the initial temperature by about 30%. The centrality dependence [11] is close to the results from AuAu collisions at RHIC, see Figure 2. This is best described by models with gluon saturation or strong shadowing effects.

4. Baryon number transport

In inelastic non-diffractive proton-proton collisions at very high energy the incoming projectile breaks up into several hadrons which emerge after the collision in general under small angles along the original beam direction. The deceleration of the incoming proton, or more precisely of the conserved baryon number associated with the beam particles, is often called baryon-number transport and has been debated theoretically for some time.

At lower collision energies the most important mechanism for baryon-number transport is the break-up of the proton into a diquark-quark configuration [12, 13] followed by hadronization of the diquark. This baryon-number transport can be quantified in terms of the rapidity loss $\Delta y = y_{beam} - y_{baryon}$. However, in this mechanism the baryon-number transport is suppressed exponentially as a function of the rapidity loss. At the LHC the accessible rapidity loss region is much larger than at

lower collision energies. Therefore the measurement of the net baryon number at mid-rapidity or equivalently the baryon to antibaryon ratio could reveal additional baryon transport mechanisms.

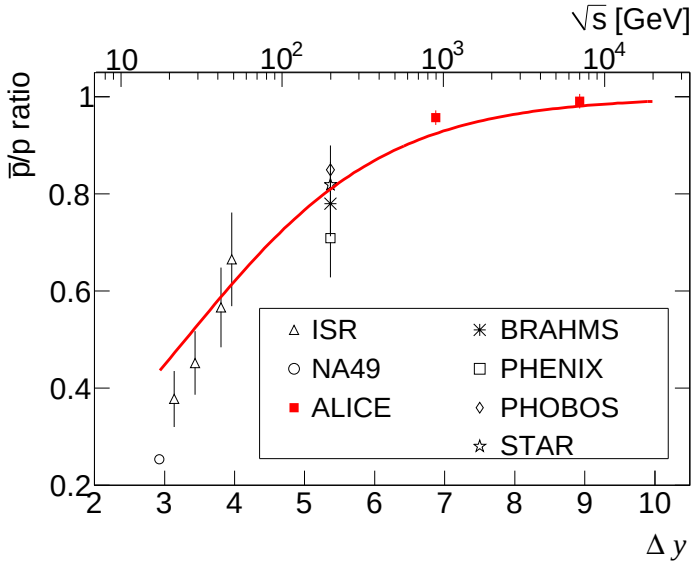

Figure 3: Figure reproduced from [15]. Central rapidity $\bar{p}/p$ ratio as a function of the rapidity interval Δy (lower axis). Error bars correspond to the quadratic sum of statistical and systematic uncertainties for the RHIC and LHC measurements and to statistical errors otherwise.

The most prominent alternative mechanism proposed is transport through a string junction. In this model the proton is assumed to consist of three valence quarks bound by strings which form a junction between them. The baryon-number can then be transported not only by the quarks but also by the string junction. Here the baryon-number transport is also suppressed exponentially but with a different slope. QCD inspired estimates [14] suggest a value for the baryon-antibaryon ratio significantly different from one at mid-rapidity at LHC energies.

Figure 3 shows the measured antiproton-proton ratio as a function of the rapidity loss comparing the ALICE results to those of other experiments at lower energies. Although the measured value at 0.9 TeV is close to one there is still a small but significant excess of protons over antiprotons. At 7 TeV the ratio is consistent with one, setting a stringent limit on the amount of baryon-transport over 9 units of rapidity. The existence of large values of the baryon-transport, as predicted by [14] is therefore excluded. The curve in figure 3 represents a fit to the data including the various baryon-transport mechanisms. The result is compatible with the assumption that only the diquark fragmentation mechanism contribute to the baryon transport. The details of this analysis are described in [15].

5. Transverse momentum spectra in pp

Perturbative Quantum Chromo Dynamics (pQCD) is a framework for the quantitative description of parton interactions at large momentum transfers. However, even at LHC energies, a large fraction of the particles produced in pp and PbPb collisions are produced in soft interactions for which pQCD is not well suited. These soft interactions are usually described using a phenomeno-

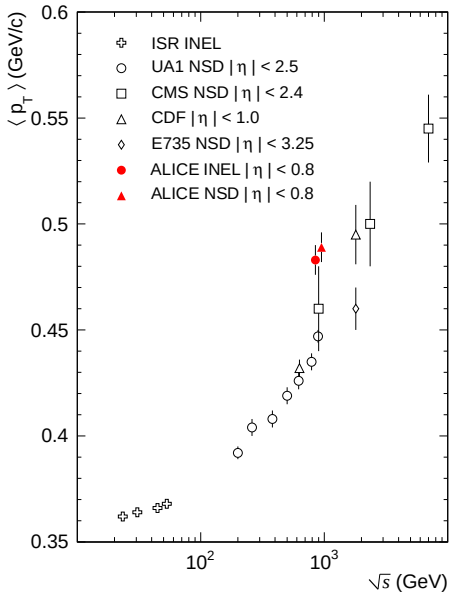

Figure 4: Figure reproduced from [16]. Energy dependence of the average transverse momentum of primary charged particles in pp and $p\bar{p}$ collisions.

logical approach. The event generators using a phenomenological approach (e.g. PYTHIA and PHOJET) need to be tuned in order to describe the particle production properly.

The inclusive charged particle transverse momentum distribution was measured [16] for pp collisions at $\sqrt{s}$=0.9 TeV. This measurement used the central detectors ($|\eta| < 0.8$) covering the p_t range from 0.15 until 10 GeV/c. For p_t below 3 GeV/c the spectrum is well described by a modified Hagedorn fit while at higher p_t the data is best described by a powerlaw [16]. The powerlaw shape of the spectrum is suggests that the pQCD approximations are applicable in this region. The average transverse momentum is $0.483 \pm 0.001(\text{stat}) \pm 0.007(\text{syst})$ GeV/c for inelastic and $0.489 \pm 0.001(\text{stat}) \pm 0.007(\text{syst})$ GeV/c for non-single diffractive events,see figure 4. These values are larger than measurements in wider pseudorapidity intervals for the same collision energy. A similar increase for a smaller rapidity window is seen for the Tevatron results in figure 4. None of the models compared simultaneously describes the p_t spectrum and the correlation between the average p_t and the multiplicity. In particular in the low p_t region the models require further tuning. Recent results for p_t spectra of identified stable charged and neutral strange particles [17, 21] show that in most cases PHOJET as well as the PYTHIA tunes are well below the data especially for the heavier particles. The ratio of Λ/K^0_S agrees with the STAR data but is below the data measured by UA1 and CDF. This difference could be due to differences in the feed down corrections applied by the experiments or in the acceptance or triggers and will be investigated further.

The measured charged particle spectra in $|\eta| < 0.8$ and 0.3<p_t<20 GeV/c in PbPb collisions at 2.76 GeV collision energy were compared to the expectation in pp collisions at the same energy, scaled by the number of underlying nucleon–nucleon collisions. For this comparison the pp results were scaled to the equivalent PbPb energy, see also [18]. The comparison is expressed in terms of the nuclear modification factor R_{AA}. Figure 5 shows the comparison of the nuclear modification factor in central collisions to the results of the PHENIX and STAR experiments. In central colli-

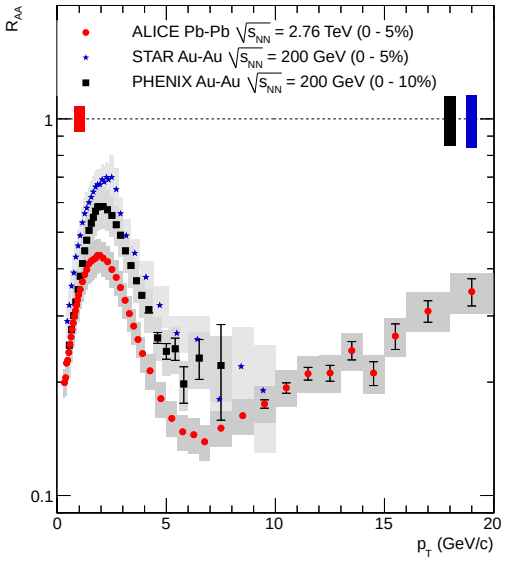

Figure 5: Figures reproduced from [18]. Comparison of R_{AA} in central PbPb collisions to measurements by PHENIX and STAR at RHIC. The error representation of the ALICE data is as in the left panel. Error bars indicate the statistical uncertainties, the boxes contain the systematic errors. For further details see text. The statistical and systematic errors of the PHENIX data are shown as error bars and boxes, respectively. The statistical and systematic errors of the STAR data are combined and shown as boxes. The vertical bars around R_{AA}=1 indicate the p_t independent scaling errors on R_{AA}.

sions, R_{AA} reaches a minimum of about 0.14 at about 6 GeV/c and the measured suppression of high p_t particles is stronger than that observed at lower collision energies, despite the much flatter p_t spectrum in pp at the LHC. The strong suppression of intermediate p_t particles suggests that a very dense medium is formed in central PbPb collisions at the LHC. At larger p_t the nuclear modification factor increases significantly. A quantitative determination of the energy loss and medium density will require further investigation of gluon shadowing and saturation in the present energy range and detailed theoretical modelling.

6. Femtoscopy

The spatial extent of the system at decoupling is accessible via intensity interferometry. This technique uses the Bose-Einstein enhancement of identical bosons emitted nearby in phasespace. The measured radii are connected to the volume of homogeneity and the system life time. This method was applied to the ALICE data from pp collisions [19] as well as to the data from PbPb collisions [20] using pions. The results in pp interactions show similar trends with respect to e.g. multiplicity or pair momentum as the PbPb results. However, the interpretation of the pp results is controversial. A systematic study of both pp and PbPb data will shed light on the nature, the similarities and the differences of their dynamics.

The product of the radii measured in PbPb collisions, see left panel of figure 6, shows a linear dependence on the charged-particle pseudorapidity density and is two times larger at the LHC than at RHIC. Within a hydrodynamic scenario the decoupling time for pions at mid-rapidity can

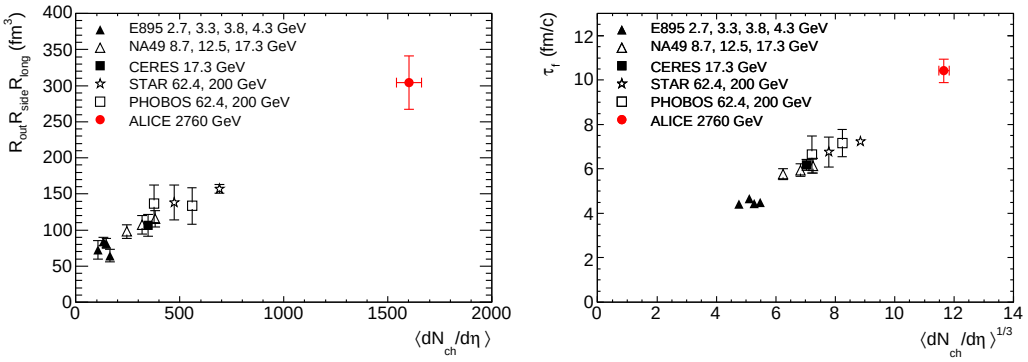

Figure 6: Figures reproduced from [20]. Left panel: Product of the three HBT radii at k_T=0.3 GeV/c. The ALICE result is compared to results form experiments at lower energies. Right panel: The decoupling time compared to results from other experiments at lower collision energies.

be estimated from R_{long} because both are connected by the longitudinal velocity gradient of the expanding system. The decoupling time extracted is shown in the right panel of figure 6 and compared to values published by experiments at lower energies. The system life time increases linearly with R_{long}, i.e. with the cube root of the charged particle pseudo rapidity as expected in the hydrodynamical scenario. A more detailed study of the radii as a function of the pion pair momentum confirms the agreement with hydrodynamical models. Within the hydro interpretation the system life time increases by about 20% with respect to the RHIC results.

7. Flow

When nuclei collide at finite impact parameter the geometrical overlap region and therefore the initial matter distribution is anisotropic. If the matter is interacting this spatial anisotropy is converted into an anisotropic momentum distribution. The second Fourier coefficient of the azimuthal distribution of the final state hadrons is called elliptic flow. For varying impact parameters of the collision the initial shape and therefore the strength of the elliptic flow varies, allowing a detailed comparison with models and extraction of the equation of state of the state produced in the collision.

The top panel of figure 7 shows the second harmonic (v_2) measured [22] using two and four particle correlations compared to measurements by the STAR experiment at RHIC. While the $v_2\{2\}(p_t)$ measurement is still biased by effects which are not correlated to the initial geometry, simulations and analytical estimates show that the $v_2\{4\}(p_t)$ measurement is essentially unbiased. The lower panel of figure 7 shows $v_2\{4\}(p_t)$ measurement for various centralities compared to the STAR measurements. The p_t dependence of the flow coefficient does not change significantly when the beam energy is increased from 0.2 TeV to 2.76 TeV. The right panel of figure 7 shows that the p_t integrated value for the 20%-30% centrality class increases about 30% with respect to the RHIC energy.

Models based on ideal relativistic hydrodynamics with zero shear viscosity and assuming an equation of state compatible with QGP formation describe the data from RHIC reasonably well. The models that describe the data at RHIC energies predict a modest increase of the p_t integrated

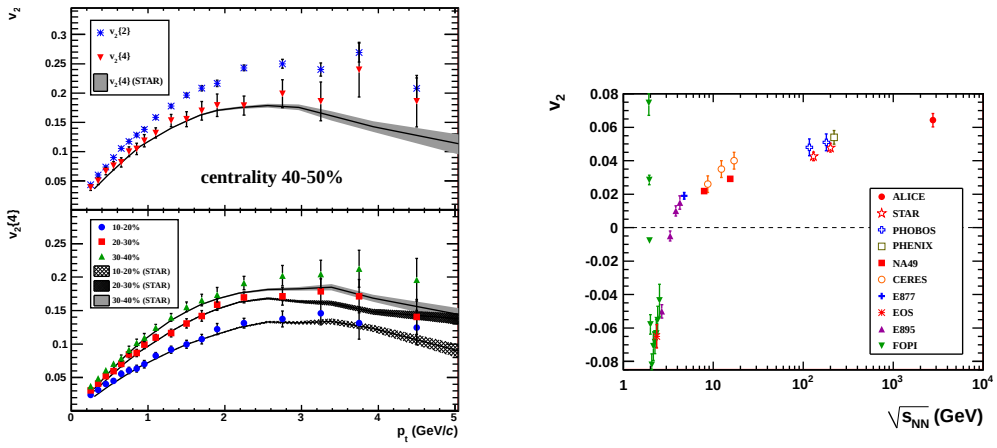

Figure 7: Figures reproduced from [22]. Top left panel: $v_2(p_t)$ for the centrality bin 40-50% from the 2- and 4-particle cumulant methods for this measurement and for AuAu collisions at $\sqrt{s_{NN}} = 200$ GeV. Bottom left panel: $v_2\{4\}(p_t)$ for various centralities compared to STAR measurements. The data points in the 20–30% centrality bin are shifted in p_t for visibility. Right panel: Integrated elliptic flow at 2.76 TeV in PbPb 20–30% centrality class compared with results from lower energies taken at similar centralities

elliptic flow at the LHC. In these hydrodynamic models the charged particle elliptic flow as a function of p_t does not change significantly. Hydrodynamic calculations show an increase of the radial flow on top of the increase of the average p_t which is also seen in pp collisions. Thus the p_t integrated flow increases due to the increase in the average p_t. This also leads to a mass dependence of the $v_2\{4\}(p_t)$ which will be measured in future analysis using the excellent ALICE particle identification capabilities.

References

[1] K. Aamodt et al., J. Instrum. 3, S08002 (2008).

[2] F. Carminati et al., J. Phys. G30, 1517 (2004).

[3] J. Alme et al., Nucl. Instr. and Meth. A 622(2010)316.

[4] K. Aamodt et al., J. Instrum. 5, P03003 (2010).

[5] P.Z. Skands, arXiv:0905.3418 (2009).

[6] R. Engel, J. Ranft, S. Roesler, Phys. Rev. D 52 (1995) 1459.

[7] K. Aamodt et al., Eur. Phys. J. C 65 (2010) 111

[8] K Aamodt et al., Eur. Phys. J. C 68 (2010) 345

[9] K Aamodt et al., Eur. Phys. J. C 68 (2010) 89

[10] K Aamodt et al., Phys. Rev. Lett. 105 (2010) 252301

[11] K Aamodt et al., Phys. Rev. Lett. 106 (2010) 032301

[12] A. Capella et al., Phys. Rep. 236, 225 (1994)

[13] G.C. Rossi and G. Veneziano, Nucl. Phys. B123 (1997) 507; X. Artru, Nucl. Phys. B85, 442 (1975); M. Imachi, S. Otsuki and F. Toyoda Prog. Theor. Phys. 54, 280 (1975);

[14] B.Z. Kopeliovich, Sov. J. Nucl. Phys. 45, 1078 (1987); B.Z. Kopeliovich, B. Povh, Z. Phys. C75, 693 (1997); B.Z. Kopeliovich, B. Povh, Phys. Lett. B446, 321 (1999).

[15] K Aamodt et al., Phys. Rev. Lett. 105 (2010) 072002

[16] K Aamodt et al., Phys. Lett. B 693 (2010) 53

[17] K Aamodt et al., arXiv:1101.4110 [hep-ex]

[18] K Aamodt et al., Phys. Lett. B 696 (2011) 30

[19] K Aamodt et al., Phys. Rev. D 82 (2010) 052001

[20] K Aamodt et al., Phys. Lett. B 696 (2011) 328

[21] K Aamodt et al., arXiv:1012.3257 [hep-ex]

[22] K Aamodt et al., Phys. Rev. Lett. 105 (2010) 252302